

A lightweight, portable MRI brain scanner based on a rotating Halbach magnet

Clarissa Zimmerman Cooley^{1,2}, Jason P Stockmann^{2,3}, Brandon Dean Armstrong^{2,3}, Matthew S Rosen^{2,3}, and Lawrence L Wald²

¹Electrical Engineering, Massachusetts Institute of Technology, Cambridge, MA, United States, ²Athinoula A. Martinos Center for Biomedical Imaging, Department of Radiology, Massachusetts General Hospital, Charlestown, MA, United States, ³Department of Physics, Harvard University, Cambridge, MA, United States

TARGET AUDIENCE: MR system engineers, and those requiring portable MRI systems

PURPOSE: We constructed and tested a portable, lightweight, low-power, permanent magnet based brain MRI scanner suitable for operation in an ambulance, battle field, sports arena, or at the patient's bedside. Our goal is to allow emergency medical teams to assess brain hemorrhage from surgical complications, traumatic brain injury or stroke to accelerate care to those requiring it. The system eliminates the need for gradient coils and power supplies thru a novel encoding method which rotates the B_0 field inhomogeneity pattern of the permanent magnet creating generalized projections similar to O-Space¹ or PatLoc² encoding. We show experimental 2D, proof-of concept images, and discuss generalization to 3D.

METHODS: A 45 kg (36cm dia. 36cm length) Halbach cylinder magnet was built with NdFeB permanent magnets (Fig. 1a)^{3,4}. The center field is 77 mT (3.285 MHz) with about 1 mT (43 kHz) field variation in the center slice FOV of 16 cm. The magnet's encoding field has a roughly hyperbolic multipolar shape (Fig. 1b) that is physically rotated around the phantom during data collection. Because the encoding field cannot be switched, a spin echo sequence is used for radiofrequency refocusing of the spins, forming a projection of the phantom at each rotation. The field maps are measured and used as prior knowledge to construct the encoding matrix. Data are collected on a TecMag Apollo spectrometer with a 250 W Tomco RF amplifier and the image is reconstructed using the iterative algebraic reconstruction technique (ART)⁵.

Accurate field maps at each rotation are critical to image reconstruction. A single row of 8 solenoidal field-probes each holding a 1-mm water-filled capillary doped with copper sulfate ($T_1=100$ ms) are used to collect field information as the magnet is rotated. The field measurements are fit using polynomial basis functions (Fig 1b). The lack of magnet shielding exposes our encoding field to external fields, the most significant being the earth's field which adds vectorially to the encoding field. This is explicitly corrected for when calculating the encoding matrix. Other external fields and magnet field drift ($\sim -1/2G/^\circ C$)⁶ are measured using an MR field probe fixed to the magnet and also incorporated into the reconstruction.

For proof of concept, imaging phantoms were made using two 1" balls of doped water (Fig. 3a and 3e). In one experiment high SNR was achieved by directly winding the TR coil around the balls of water. In another experiment we used a volume Tx coil and an array of 4x 6.5cm dia. loop coils for Rx. In both case short, high power excitation pulses (125 W for a 50 μ s refocusing pulse) were necessary to cover the bandwidth of the encoding field.

RESULTS: Fig. 2 shows an example set of rotated field maps and the corresponding projections from the phantom. Fig. 3b is the reconstructed image of the same phantom using the Rx single coil. The data consisted of 128-average spin echoes with TR/TE = 200ms/9.4ms and 40 kHz readout bandwidth. Eighty projection directions were used. Fig. 3c shows the same reconstructed phantom imaged using 4 surface coils, 24 projection angles, 256 averages, and TR/TE = 200ms/20.4ms. Fig. 3d shows a simulated reconstruction with the same parameters as Fig. 3c. Fig. 3f and 3g show the experimental and simulated single coil image from the phantom in Fig. 3e (w/ 128 averages of 35 projection angles). Unlike the first phantom, there is a ball in the center of the encoding field. Because of the approximately quadrupolar symmetry of the encoding field, 90 deg of field rotation is sufficient to capture all unique projections of the object.

DISCUSSION: Blurring throughout the image is greatly improved by the external field and temperature drift corrections, but some obvious artifacts remain. In Fig. 2b, the balls are located in the top half of the phantom, but we clearly see aliasing in the reconstructed images. This is expected because of the non-bijectionality of the encoding field¹. The problem is resolved in Fig. 2c-d, in which the coil sensitivities from a 4 channel coil array are used to remove the ambiguity between frequency-matched isocontours in different quadrants. Blurring in the center is seen in Fig. 3f-g. Similar to Patloc imaging, the resolution of the images is lowest in the center because of the low field variation in that area. We propose shifting the encoding field off-center from the rotation axis (using shims) to address this, similar to O-Space imaging².

CONCLUSION: These initial images and simulations are a 2D proof of concept for imaging in a rotating inhomogeneous field without additional gradient coils. Signal-to-noise ratio would benefit from RF shielding of the magnet and/or coils. Image reconstruction would be simplified if the temperature of the magnet could be regulated. However, this could limit portability of the system, and we have shown that these inconveniences can be mitigated by careful field calibration before imaging and field drift monitoring during imaging. Current work includes continued improvements to the field map calibration to decrease blurring and the use of more and higher sensitivity receive arrays. The use of Transmit Array Spatial Encoding (TRASE)⁷ is also being implemented for slice localization in the longitudinal direction to enable 3D imaging.

REFERENCES: (1) Schultz G, IEEE Trans Med Imag 2011. (2) Stockmann, MRM 2010. (3) Zimmerman C ISMRM 2012. (4) Halbach K, Nucl Instr Meth 1980. (5) Herman G, Comp. Biol. Med. 1976. (6) Campbell P, Permanent Magnet Materials & their Application, 1994. (7) Sharp J, MRM 2010. **ACKNOWLEDGMENTS:** The authors wish to thank Cris Lapierre, Mathieu Sarraclanie, James Blau, and Eli Siskind for their help. This research was supported by DoD/USAMRRA W81XWH-11-2-0076 (DM09094).

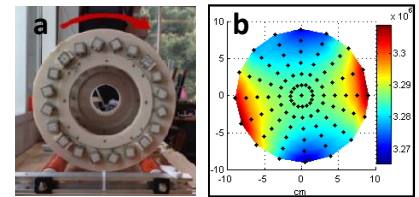


Figure 1: (a) magnet on high friction rollers, (b) interpolated field map in Hz, black dots are the field probe positions.

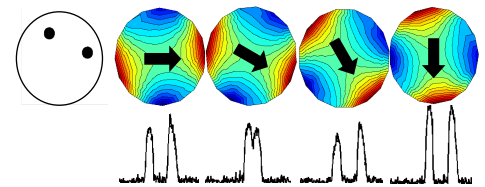


Figure 2: Six representative encoding field rotations and experimental projections of phantom on left (1 coil, 128 averages, SNR ~ 30). Arrow is B_0 direction.

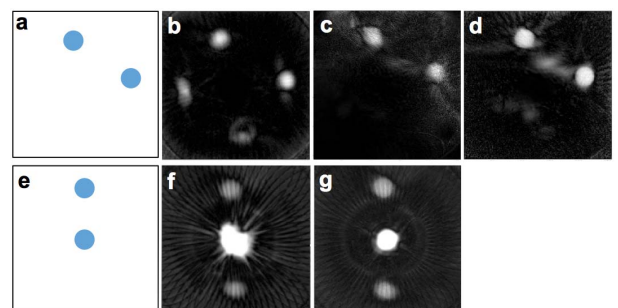


Figure 3: (a) ball locations in ground truth phantom 1, (b) 80 projections of phantom 1 using one solenoid receive coil (c) 24 projections of phantom 1 using 4 receive coils, (d) simulated version of Fig. 3c, (e) ground truth phantom 2, (f) 35 projections of phantom 2 using one coil, (g) simulated version of Fig. 3f. Field of view is 16 cm in all images.